Finite Element Computations Involving Creep Combined With Other Nonlinearities

G. Panosyan, J. Beziat, E. Carnoy
Novatome, 20 av. Edouard Herriot, F-92350 Le Plessis-Robinson, France

ABSTRACT

Creep is an essential parameter of LMFBR Components operating under high temperatures. In particular the utilisation of steels for short times with respect to their creep capacity requires a numerical model which integrates in a reliable way the primary creep.

The algorithmes elaborated will briefly described, with particular emphasis on the following points : creep-plasticity combination, stability of various integration schemes and method to compute hold time increments during creep and relaxation.

In the models adopted and examples presented, plastic and creep strains develop in conjunction, since some experimental results proved this to be necessary.

The numerical examples presented mainly concern primary creep coupled with plasticity and are divided in three groups :

- Applications designed to validate creep schemes in the main types of load conditions encountered and creep-plasticity interaction.
- Inclusion of creep in design of structures subjected to high temperatures and cyclic loads, in order to combine cyclic fatigue and creep.
- Numerical aspect of creep during a comparative study of computational experimental results on small notched specimens.

1. Introduction

The primary creep is characterized by a quick variation of the creep strain rate. For the creep time to be considered, most stainless structures that are employed in LMFBR components do not reach the secondary creep behavior. Therefore, it has been necessary to assess primary creep strains accurately. The large variation of the creep strain rate at the beginning of the process introduces difficulties within the calculation and suitable algorithmes have had to be developed, which have been presented elsewhere.

The secondary creep characterized by a stationary period at constant rate is predominant in most metals. Thus, it has been taken into account, while numerical difficulties are much less in this respect.

In the considered models, creep strains can develop themselves with plastic strains, simultaneously. In the present time, our researches consist in defining from experimental data a material model suitable for industrial applications and which takes into account the interaction between creep and plasticity.

2. Choice of creep model

Two types of creep laws are integrated in our development :

. Primary and secondary laws applicable to steels used in LMFBR components and automatically integrated.

. Norton-Odqvist type primary and secondary general laws.

In what follows, we shall only consider laws of the first type, of which the secondary part is also Norton type.

Since the equivalent creep strain is given for primary creep, by :

$$\varepsilon^c = C_1 t^{C_2} \bar{\sigma}^{n_1} \qquad \text{with} \qquad t < t_{ep} \tag{1}$$

where t_{ep} designates the end of primary creep

$$t_{ep} = C_3 \bar{\sigma}^{n_3} \tag{2}$$

In the multiaxial case, the creep rate tensor and stress deviator are assumed to be colinear / 1 , 3 , 4 /.

$$\dot{\varepsilon}^c_{ij} = \frac{3}{2} \frac{\dot{\bar{\varepsilon}}^c}{\bar{\sigma}} s_{ij} \tag{3}$$

The equivalent strain rate is derived from (1)

$$\dot{\bar{\varepsilon}}^c = C_1 C_2 t^{C_2 - 1} \bar{\sigma}^{n_1} \tag{4}$$

In equation (4), the creep rate depends only on time and on the equivalent stress (time hardening model). However, it has been experimentally shown that the material behaviour is better described by the strain history and that consequently, strain hardening is better adapted to the analysis of material subjected to variable stresses and cyclic loading.

Eliminating time from equation (4)

$$t = \left(\frac{\bar{\varepsilon}^c}{C_1 \bar{\sigma}^{n_1}} \right)^{1/C_2} \tag{5}$$

In this case, we derive the expression of the equivalent creep rate, depending on the equivalent creep strain and the stress level.

$$\dot{\bar{\varepsilon}}^c = C_1^{1/C_2} C_2 \, \bar{\varepsilon}^{c\,(C_2-1)/C_2} \, \bar{\sigma}^{n_1/C_2} \tag{6}$$

The strain hardening model can lead to difficulties in the event of load reversal /3/.

Although no provision is made in our algorithm for extension of the model to cover unloading cases /3/, we shall discuss in the numerical examples, a method for the inclusion of creep during a cyclic loading.

3. Constitutive laws

Creep is subsequently integrated in the constitutive equations as described below.

If small strains are assumed, and creep-plasticity interaction is neglected, the incremental relation is based on an infinitesimal stress increment.

$$\Delta \sigma_{ij} = D_{ijkl} \, (\bar{\sigma}, t, \bar{\varepsilon}^c) \, \varepsilon_{kl}^{mech} \tag{7}$$

where D_{ijkl} is the tangent elasto-plastic matrix and,

$$\Delta \varepsilon_{ij}^{mech} = \Delta \varepsilon^T - (\Delta \varepsilon_{ij}^{th} + \Delta \varepsilon_{ij}^c) \tag{8}$$

with $\Delta \varepsilon_{ij}^{th}$ as thermal strains.

The numerical integration technique is detailed in /5, 2/. When creep occurs, one calculate the stress state corresponding to a given total strain increment. The advantage of this technique is that plasticity and creep develop jointly. In other words, creep strains can induce local elasto-plastic redistribution, which is in accordance with experimental results.

By linearization of (3) and (4) and with

$$\Delta \varepsilon_{ij}^c = \int_{\Delta t} \dot{\varepsilon}_{ij}^c \, d\tau \tag{9}$$

one gets, after a few manipulations, the following time hardening equation :

$$\Delta \varepsilon_{ij}^c = \dot{\varepsilon}_{ij}^c \, (\bar{\sigma}, t, \bar{\varepsilon}^c) \Delta t + F_{ijkl} \, (\bar{\sigma}, t, \bar{\varepsilon}^c) \, \Delta \sigma_{kl} \tag{10}$$

$$= \Delta \varepsilon_{ij}^{co} + F_{ijkl} \, \Delta \sigma_{kl} \tag{11}$$

4. Computation of creep strain increments

In order to calculate the increase in creep $\Delta \varepsilon_{ij}^c$, four one-step integration schemes have been considered, with explicit shape of $\Delta \varepsilon_{ij}^c$ varying according to the scheme used and to the hardening type.

The definition and characteristics /10, 11/ of these integration schemes are as follows:

. One step implicit scheme

In this scheme, $\Delta\varepsilon_{ij}^{co}$ and F_{ijkl} are constant and dependent on the stress state at the beginning of the Δt interval. This non-iterative scheme is both stable and accurate and consequently more economical than those mentioned below, for reasonable Δt values.

. Implicite iterative scheme

The creep rate is assumed constant over Δt interval and equal to its value at the end of the interval.

$\Delta\varepsilon_{ij}^{co}$ and F_{ijkl} are reassessed by successive iterations, according to the stress state at the beginning of the iteration. With this scheme large Δt's can be defined, Unconditionally stable /6/, this scheme is iterative even in linear elastic cases.

. Mid-point scheme

The creep rate is constant on Δt and equal to its value calculated at point ($\sigma_{ij} + \Delta\sigma_{ij}/2$; $t_1 + \Delta t/2$), t_1 designating the time at the beginning of the Δt interval. The characteristics of this scheme are similar to those of previous one. For linear cases, it is the most accurate method.

. Euler scheme

The creep rate is maintained equal to its value at the beginning of the Δt interval. In this case, F_{ijkl} is identically null. Although non iterative, this conditionnally stable scheme has the disadvantage of necessitating very small Δt values /7/.

In the case of strain hardening, the creep rate is defined in terms of equivalent strain , assuming that the equivalent creep strain defining the hardening, is that existing at the beginning of the time interval considered. We thus, revert to the previous case, defining a pseudo-time at the beginning of the interval, as expended in (5).

$$t^*_1 = \left(\frac{\bar{\varepsilon}_c}{C_1 \bar{\sigma}^{n1}} \right)^{1/c_2} \qquad (12)$$

As regards the choice of creep time steps, we have proposed two approaches in the cases of constant stress and imposed total strain (relaxation), which utilize the stability of the previous schemes both in time and strain hardening cases.

5. Numerical examples

The applications investigated are classified in two groups. The first group comprises simple cases of creep subsantiation, associated with the main types of loading encountered : imposed strain, imposed strain rate, creep-plasticity combination. Constant stress type has been fully discussed /11/. In these cases, the reference solutions are obtained by numerical integration, using a 7^{th} order Runge-Kutta method with very small time steps. For the creep-interaction example a theorical solution is proposed. The second group of examples concerns the elasto-plastic creep ahalysis of structures subjected to complex loadings. The first example shows a metnod used to solve a creep-fatigue problem in a case of cyclic loading. In the second example, visco-plastic calculations are used to check the results of tests performed on notched specimens, subjected to axial loading and then to creep times.

5.1 Relaxation under imposed strain

An uniaxial state is imposed to a specimen (figure 1). The longitudinal strain is fixed. We analyse the relaxation of longitudinal stress after the specimen has been subjected to primary creep during 5 hours. In this example, time hardening model is used consisting, first of applying ten constant 0.5 h time steps. The pure implicit and mid point schemes give the best results (figure 1). The calculation is resumed and the time steps are estimated using formulation in /11/ with $\beta = 0.1$.

$$t_{1\cdots\cdots 8} = 0.0488 \ ; \ 0.0680 \ ; \ 0.139 \ ; \ 0.270 \ ; \ 0.446 \ ; \ 0.820 \ ; \ 1.310 \ ; \ 1.900$$

The accurate results obtained by the implicit one-step and mid point schemes are shown in figure 2.

5.2 Creep under imposed total strain rate

An uniaxial stress state is imposed to a specimen with a given strain rate (figure 3). The evolution of stress versus strain is analysed for primary creep during 5 hours. In this example applying strain hardening, two calculation methods have been adopted.

The first consists in seeking solutions with 10 equal steps. It can be seen in figure 3 that solutions calculated by the different schemes used correspond to the theoretical solution.

In the second, we adopted five 1 hour time steps (figure 4). The implicit one step scheme induces strong oscillations. It can be noted that, despite very large Δt values, the implicit and mid-point scheme give good results.

5.3 Creep-plasticity interaction

The purpose of this example is to validate the solution algorithm in case where creep involves elastoplastic distribution. The structure considered is constitued by 2 bars (figure 5). By arranging the elastoplastic characteristics of the two bars and assuming equal displacements for both of them, we obtain the following phenomenon :

- during loading, bar 1 plastifies and bar 2 remains elastic. During creep, imposing the same creep characteristics for both bars, bar 1 unloads and bar 2 plastifies. This phenomenon should stabilize and the stresses will tend towards the same limit if the cross-section of the bars is the same.

The theoretical solution is discussed in /14/. The Limite Element model employs two plane stress quadrilateral elements having the same geometrical location. Limit conditions are imposed to ensure homogenous strain in both elements.

A 10 - step and then 5 - step solutions were used to solve the equation. The results are given in figure 6. The conformity between the analytical solution and the calculations demonstrates the accuracy of the algorithme in case of creep-plasticity interaction.

5.4 Creep in a steam generator penetration nozzle subjected to cyclic thermomechanical loading

In this example, we describe a method for the assessment of creep damage in structures subjected to cyclic loadings (figure 7). The purpose of this example is not to emphasize the calculation results /13/, but rather to describe the method used, which permits creep

application in cases of load reversal. The structure considered is a steam generator penetration nozzle subjected to piping induced stresses during thermal transients. The characteristics of the material are as follows :

- The strain hardening law is kinematic, with material characteristics varying with temperature.
- The creep law is a Norton-Odqvist type ; the operating conditions situate the structure in primary creep behaviour.

The mechanical loading consists of an internal pressure and the forces applied on the nozzle.

The thermal transients, calculated previously by a thermal analysis code, induce also time dependant temperatures through the thickness at the integration points. The calculation covers two thermal envelopping cycles, with a large number of elastoplastic steps (figure 8). The load analysed is an envelop integrating normal and disturbed situations. The results were checked in accordance with the requirements specified in Code Case 47 or RAMSES recommendations / 15 /.

. stress limits due to mechanical loadings,
. ratcheting
. fatigue damage
. creep damage and fatigue - creep interaction.

The envelopping transients are equidistant during time, with maximization of the residual stress σ_R at the end of the envelop, which maximizes the creep damage. This procedure is advantageous in that the load cycles are extremely shorts compared to the hold time. We are presently elaborating a cyclic viscoplastic law. But the use of such laws for this type of calculations remains, even so, highly hypotetical, since the load increments have to be small, which is computer time consuming. Furthermore, the fact that these laws depend on the strain rate makes them very delicate to handle.

4.5 Tests - computation comparison on notched specimens

Tests were performed on axisymmetric notched 316 SS specimens to study the effects on creep damage and creep fatigue interaction of triaxiality of stresses. Although the ultimate aim of the survey was to elaborate a creep damage model in conformity with the numerical results obtained / 12 /. In this example, we only emphasize the good agreement that is obtained between experiment and finite element calculations inculding creep. Two geometries were used (5 mm and 1 mm notch radius). The specimens were meshed with 2D isoparametric 8-node elements and represented on 1/4 for reasons of symmetry (figure 9). Geometrical nonlinearities are taken into account (Updated Lagrangian). For the elastoplastic part, a multilinear isotropic hardening law is applied. Comparison over the loading period (0-375 Mpa for the first specimen and 0-404 Mpa for the second) shows good agreement between tests and calculation results (figures 10 and 11), with strains becoming relatively large in both cases ($\sim$ 8 %).

Primary and secondary creep analysis was applied with a strain hardening model using mid-point scheme. The respective hold time of 1000 and 700 hours were applied in 1 % strain range (figures 12 and 13). On $\bar{\varepsilon}$ and longitudinal elongation, calculations and experiments differ by about 15 %. Despite the limited number of tests, the comparisons can be considered as satisfactory. The calculations were resumed with a higher stress level. In this case, the strains become more significant and the correspondance between results and experiment is less good. This is mainly due to creep rate dispersion during the experiments : the difference between the creep law derived from uniaxial data and the experimental points obtained on the specimens explains the difference between tests and calculations. Under these conditions stress redistribution during creep can be considered as satisfactory.

In conclusion, the numerical part of this experiment demonstrates the efficiency of the algorithms developped in cases of pronounced material and geometrical nonlinearities and creep. Present trends in our investigations concern the definition of viscoplastic laws, taking into account the incidence of creep on hardening parameters.

REFERENCES

1. : RASHID, Y.R.,
"Analysis of two dimensional problems under simultaneaous creep and plasticity"
GEAP-10546, AEC Research and Development Report, January 1972

2. : NYSSEN, C.
An efficient and accurate iterative method, allowing large incremental steps, to solve elasto-plastic problems, symposium on computational methods in non linear Structural and Solid Mechanics, Washigton (1980)

3. : GREENSTREET, W.L., CORUM, J.M., PUGH, C.E. and LIU, K.C.
"Currently recommended constitutive equations for inelastic design analysis of FFTF components"
Oak Ridge National Laboratory, TM-3602

4. : DONEA, J.
"The Application of computer Methods to Creep Analysis" in "Creep of engineering Materials and Structures"
Ispra, November 1978

5. : NYSSEN, C.
"Modélisation par éléments finis du comportement non linéaire de structures aérospatiales"
Thèse de doctorat, Université de Liège, 1979

6. : HUGUES, T.J.R. and TAYLOR, R.L.,
"Unconditionally stable algorithms for quasi-static elasto/visco plastic finite element analysis"
Comp. and Struct. Vol. 8, pp. 169-173, 1978

7. : CORMEAU, I.,
"Numerical stability in quasi-static elasto/visco-plasticity"
Int. J. for Num. Meth. in Eng., Vol. 9, pp 109-127, 1975

8. : SUTHERLAND W.H.
"Finite element computer code for creep analysis"
Nuclear Eng. and Design, 11, pp 269-285, 1969

9. : WILLIAM, K.J.
"Numerical solution of inelastic rate process"
Comp. and Struct., Vol. 8, pp 511-531, 1978

10. : NOVNL, Analyse non linéaire statique et dynamique de structures,
NOVATOME technical note MSD 80.039

11. : NYSSEN, C., PANOSYAN, G., BEZIAT, J.
"Comparison of one step implicit integration schemes for creep analysis using the finite element method"
SMIRT VI, Paris (1980), M 3/2

12. : BEZIAT, J., DIBOINE, A., LEVAILLANT, CH., PINEAU A.
"Creep Damage and Fatigue Creep Interaction in a 316 SS under triaxial Stresses"
ASME PVP Division conference Orlando (1982)

13. : NOVATOME technical note MSD 79.045

14. : NOVATOME technical note CDD 83.038

15. : RAMSES, Note 40 702

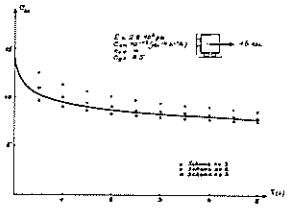

Figure 1 : Relaxation under imposed strain (constant time interval)

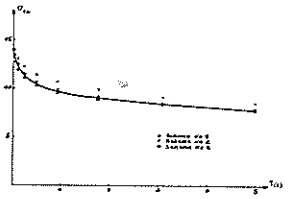

Figure 2 : Relaxation under imposed strain (computed time interval)

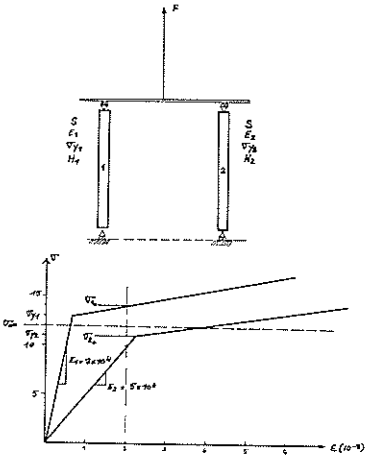

Figure 5 : Creep-plasticity (geometry, tensile curve)

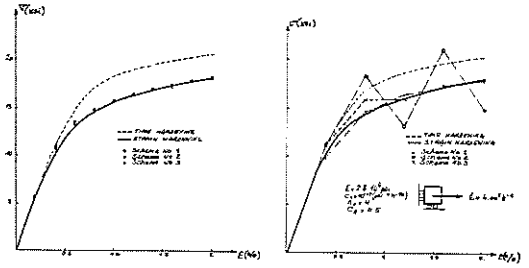

Figure 3 : Creep under imposed total strain rate (10 time steps)

Figure 4 : Creep under imposed total strain rate (4 time steps)

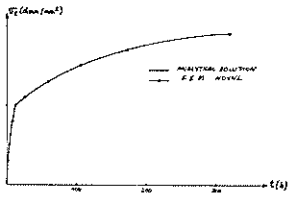

Figure 6 : Creep-plasticity ($\dot{\sigma} = g(t)$ curve)

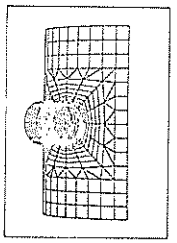

Figure 7 : Steam generator nozzle (geometry)

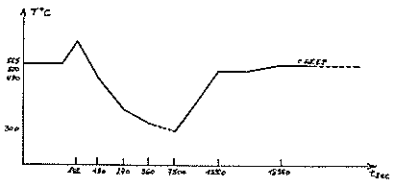

Figure 8 : Steam generator nozzle (loading curve)

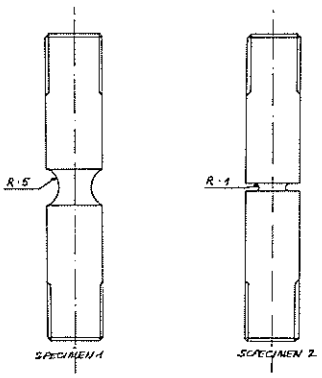

Figure 9 : Notched specimen (geometry)

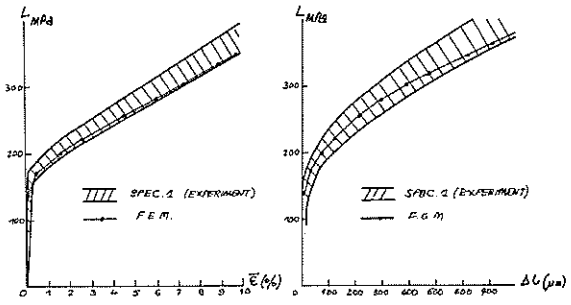

Figure 10 : Notched specimen (comparison during loading)

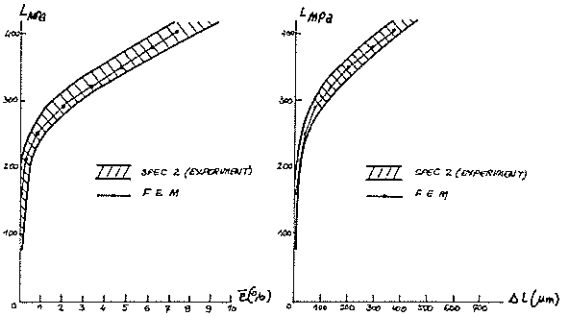

Figure 11 : Notched specimen (comparison during loading)

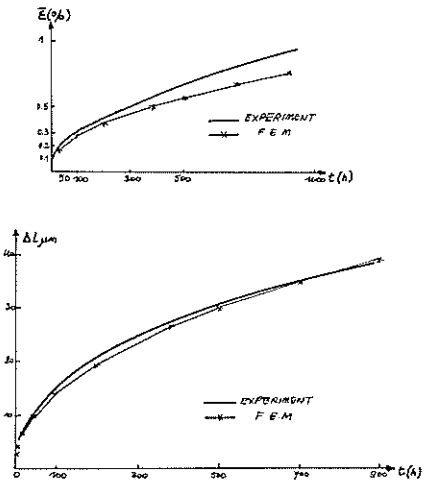

Figure 12 : Notched specimen (comparison during hold time)

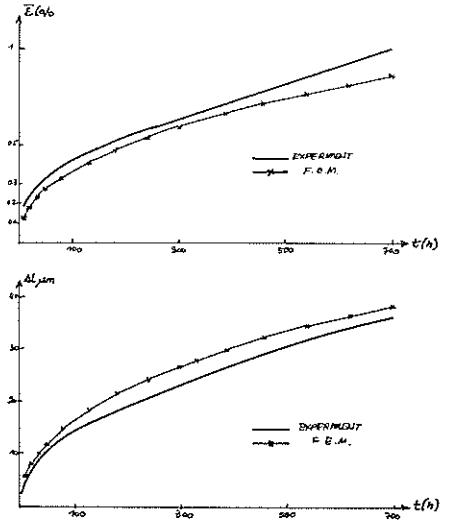

Figure 13 : Notched specimen (comparison during hold time)